

Selected aspects of the classical molecular dynamics of N bodies in strong interaction.

D. Cussol

LPC Caen (IN2P3-CNRS/ISMRA et Université), 14050 Caen Cedex , France

(Dated: November 1, 2018)

Selected results of a classical simulation of N bodies in strong interaction are presented. The static properties of such classical systems are qualitatively similar to the known properties of atomic nuclei. The simulations of collisions show that all observed reaction mechanisms in nucleus-nucleus collisions are present in this numerical simulation. The first studies of such collisions are in qualitative agreement with experimental observations. This simulation could shed a new light on energy deposit in heavy ion collisions: the excitation energy of each cluster is found lower than the energy of the less bound body in the cluster. Finally, the similarities of fragmentation pattern with those obtained with a statistical code indicate that an unambiguous link can be established between the statistical and the dynamical descriptions of reaction mechanisms.

PACS numbers: 24.10.Cn, 25.70.-z

Keywords: Classical N-body dynamics, nucleus-nucleus collisions, reaction mechanisms

During the last decades, heavy ions collisions have been widely used and intensively studied experimentally to determine the equation of state of nuclear matter. Many reaction mechanisms have been identified and a lot of theoretical works has been induced. Schematically, the incident energy domain has been divided in three parts: the low energy range, up to 10~20 A.MeV, where fusion and deep inelastic processes are dominant; the high energy range, above 100 A.MeV, where the nucleonic and sub-nucleonic degrees of freedom start to play a significant role; and the intermediate energy range, from 20 A.MeV to 100 A.MeV, where binary processes and multi-fragmentation take place. At each energy range, the reaction is schematically described as a two steps process: an entrance channel during which excited nuclei are formed, and a decay stage where the excited fragments cool down by particle or fragment emissions.

Theoretically, the entrance channel of the reaction is mainly described by dynamical models. At low energy, the attractive character of the interaction is dominant and the entrance channel is described mainly by mean-field approaches [1]. At high energies, the repulsive part of the interaction and its nucleon-nucleon character are dominant and cascade models are mainly used to describe the first moments of the collision [2]. At intermediate energies, the attractive part and the repulsive part of the interaction interfere. Transport models are widely used to describe the entrance channel at this energy range [3, 4, 5, 6, 7, 8, 9]. They contain a mean-field part through the one-body evolution of the system, and a nucleon-nucleon part through the collision term. At all energy ranges, the decay stage is mainly described by statistical decay models (GEMINI [10], SIMON [11], SMM [12], MMMC [13], QSM [14], EES [15], etc.) which assume that the nuclei formed during the first dynamical step are equilibrated.

With this scheme, it is very hard to have a global and consistent description of nucleus-nucleus collisions. Although the nucleon-nucleon interaction is the same,

whatever the incident energy and whatever the reaction time, different models are used depending on the energy range and the reaction time. The links between these different models are not obvious. For example how the liquid-drop parametrisation used in the statistical decay code can be deduced from the parameters of the interaction used in a transport code? What is the link between the incompressibility modulus of nuclear matter K_∞ and the nucleon-nucleon cross section σ_{nn} ? Is the statistical description still justified when the thermalisation time is close to or longer than the life time of excited nuclei?

The present status results mainly from the impossibility to solve the full nuclear many-body problem. To solve it, approximations are made, depending on the energy range and on the reaction time. Even after simplifications, the resulting equations do not have analytical solutions and they are often solved numerically. It seems hard nowadays to connect these different models to have a global description of the processes involved in nucleus-nucleus collisions.

Nevertheless, some attempts were made to describe globally nucleus-nucleus reactions at intermediate energies by using (semi-)classical molecular dynamics codes [16, 17, 18, 19, 20, 21, 22]. The main advantage of these codes is that the classical many-body problem can be solved numerically with a high accuracy without any assumption. The main drawback is that the quantum character of the system is ignored. A lot of work has already been done with the help of such codes to study the mechanism of fragment formation in multi-fragmentation. Could these codes do better by describing the whole reaction process, from the very beginning of the reaction up to the decay stage? Are they able to make a link between the different energy ranges? Which processes are accessible with the simplest hypothesis?

This paper will show that classical molecular dynamics simulations are interesting tools to establish the links between the different approaches used in nucleus-nucleus collision. In the first section, the Classical N-Body Dy-

namics code will be briefly described. The static properties of stable N-body systems will be studied in the second section. Some examples of reaction mechanisms and some analyses of cluster-cluster collisions are given in the third section. Finally, conclusions will be drawn.

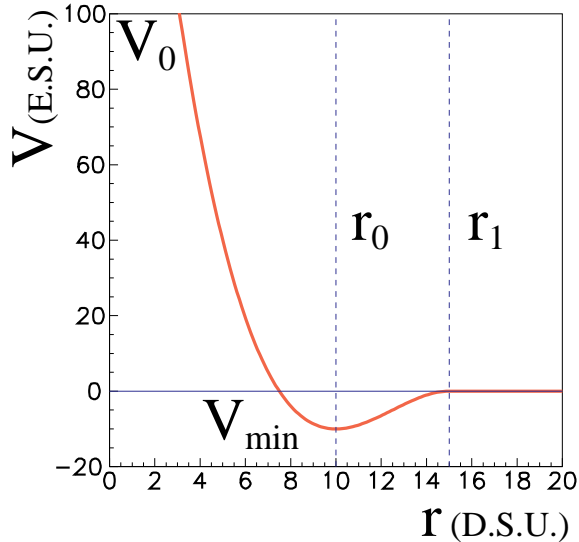


FIG. 1: Shape of the interaction used in the CNBD simulation

I. DESCRIPTION OF THE CODE.

Let us start by describing the Classical N-Body Dynamics code (labeled CNBD) used in this article. The basic ingredients of such a code are very simple. The dynamical evolution of each body of the system is driven by the classical Newtonian equations of motion. The two-body potential used in the present work is a third degree polynomial whose derivatives are null at the range r_1 and at the distance of maximum depth r_0 . The depth value is V_{min} and the value at $r = 0$ is finite and equal to V_0 . The shape of the two-body potential is shown on figure 1. This potential has the basic properties of the Lennard-Jones potential used in other works [21, 22]: a finite range attractive part and a repulsive short range part. To follow the dynamical evolution of the system an adaptative stepsize fourth-order Runge-Kutta algorithm is used [23]. The main difference with other works is that the time step Δt can vary: if the potential varies strongly, Δt is small and when the potential varies gently, Δt becomes larger. This allows a very high accuracy with shorter CPU time than for fixed time step algorithms. It requires an additional simulation parameter ϵ which is adjusted to ensure the verification of conservation laws (energy, momentum, angular momentum) with a reasonable simulation time. For an ϵ value of 10^{-5} , typical CPU times for a collision of two clusters with 50 particles each with an ending time equal to 200 time simulations units

on a Compaq DS20 computer under the UNIX True64 operating system ranges from ≈ 30 to ≈ 400 seconds, depending mainly on the impact parameter. The energy gap between the beginning and the ending simulation time is lower than 0.001%. This simulation has five free parameters: four linked to the physics (the interaction) and one linked to the numerical algorithm (ϵ).

Since one wants to study the simplest case, neither long range repulsive interaction nor quantum corrections like a Pauli potential have been introduced [24]. Additionally, no statistical decay code is applied on the excited fragments formed during the collision. The final products have to be regarded as “primary” products which will decay afterwards.

In order to avoid any confusion with nuclear physics, the units used here are called Simulation Units and noted $S.U.$. The distance will then be in Distance Simulation Units ($D.S.U.$), the energies in Energy Simulation Units ($E.S.U.$), the velocities in Velocity Simulation Units ($V.S.U.$) and the reaction time in Time Simulation Unit ($T.S.U.$). We will be only interested in the relative evolutions of the observables and in their link to the properties of the stable systems. The main goal of the present work is not to reproduce the experimental data of nucleus-nucleus collisions, but rather to see to which extent this simple simulation is qualitatively similar, or not, to experimental data.

II. STATIC PROPERTIES OF “GROUND STATES”.

Once the basic ingredients are defined, one can build stable systems. Since the two-body potential only depends on the distance between the two bodies, such systems are small crystals. The “ground states” of such systems are defined as the configuration in position space which minimizes their total energy. This is obtained by using a Metropolis simulated annealing method [23]. The locations of particles obtained this way are very close to those obtained by using a basin-hopping algorithm for Lennard-Jones clusters [25].

On top-left of figure 2 is displayed the energy per body E_{Bind}/N of these “ground states” as a function of the number N of bodies in the cluster (solid line). The dashed and dotted line corresponds to a fit using a liquid-drop formula. The dashed line corresponds to the energy of the less bound body $E_{LessBound}$ in the cluster. It will be seen that this energy seems to play a particular role in cluster-cluster collisions. The overall dependence of E_{Bind}/N with N is very similar to what is seen in nuclear physics. The main difference is seen for high values of N because of the absence of a Coulomb-like interaction: E_{Bind}/N continues to decrease with N whereas it increases for nuclei. These values are close to those found by using the basin-hopping algorithm [25].

The dependence with N of the root mean radius $r(N) = \sqrt{\langle r^2 \rangle}$ of N-body clusters is shown on the

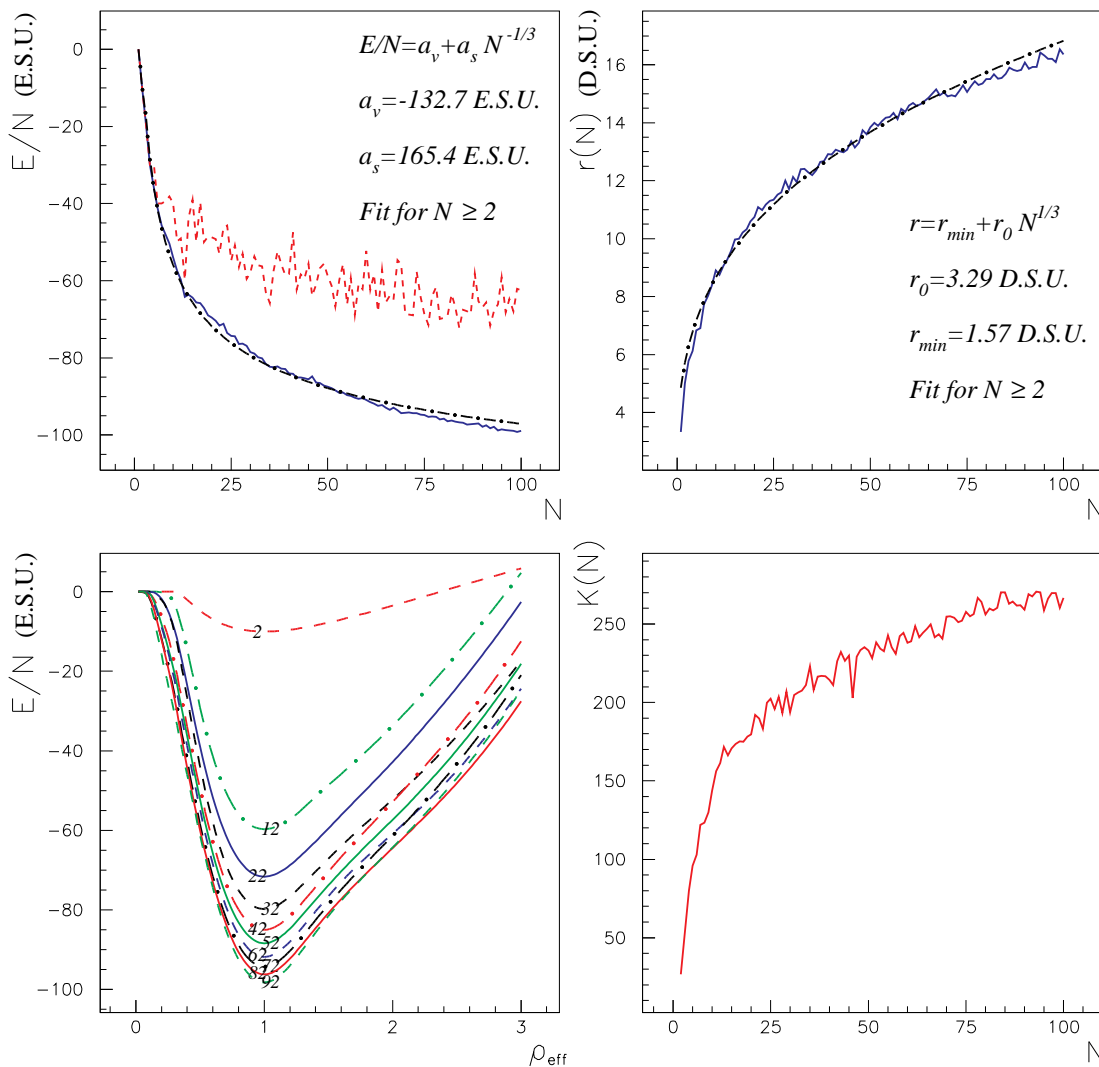


FIG. 2: Energy per body (upper left panel) and root mean square radius (upper right panel) of N -body clusters as functions of N . For these two panels, the full line correspond to the obtained values and the dashed and dotted line to a fit. On the left panel, the dashed line corresponds to the energy of the less bound body in the cluster. Lower row: zero temperature “equation of state” for different N values (left) and “incompressibility modulus” as a function of N (right).

top-right panel of figure 2 (solid line). The dashed and dotted line corresponds to a fit using a $N^{1/3}$ term. Here again, this is similar to what is known for nuclei. The main difference is the r_0 term which is due to the large size of the “repulsive core” compared to the range of the attractive part of the interaction.

Since a size can be defined, an effective density can be calculated. One can stretch and squeeze the N -body cluster and build an effective “zero temperature equation of state”. This is displayed on the low-left panel on figure 2 for various system sizes. The density ρ_{eff} on this abscissa is the density relative to the density for the “ground state”. The curvature of this “equation of state” can be computed and defined as the “compressibility modulus” $K(N)$ of the system. Its variations with N are displayed on the low-right panel of figure 2. One can

see on these two plots that the “equation of state” and $K(N)$ are strongly dependent on N for values of N below 20~30 and then less dependent on N above. One could be able to define an “equation of state of infinite matter” by computing the limit of these evolutions for huge values of N . Here again, the behavior of these classical N -body systems is very similar to that of nuclei.

This first study shows that the classical N -body clusters have strong similarities with atomic nuclei. This suggests that all the parametrisation used to describe nuclei (liquid drop parametrisation, radii, equation of state, etc...) could be directly deduced from the parameters of the two-body interaction. Since this interaction remains unchanged, the differences seen for different clusters has to be attributed only to N and to the geometrical configuration of the bodies in the clusters.

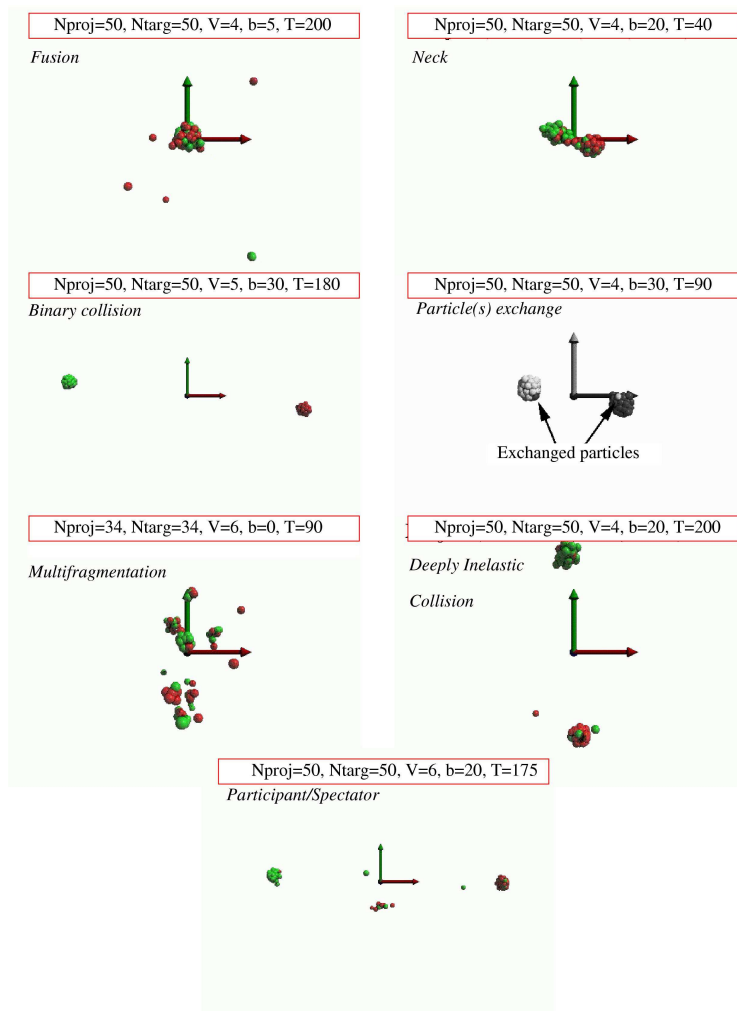


FIG. 3: Pictures of cluster-cluster collisions for different reaction mechanisms. On each panel, N_{proj} is the projectile size, N_{targ} the target size, V the relative velocity in $V.S.U.$ between the target and the projectile, b the impact parameter in $D.S.U.$ and t the collision time in $T.S.U.$.

III. CLUSTER-CLUSTER COLLISIONS.

After studying the static properties of stable N -body systems, collisions between clusters can be investigated to see what kind of reaction can be obtained. Roughly 20,000 collisions have been generated for different system sizes, different entrance channel asymmetries and different impact parameters. For each collision, the orientation of the inertia axis of clusters are randomly chosen. This avoid to run twice the same collision if the impact parameter, the target and the projectile size and the incident energy are the same for two different collisions. The simulations have been performed for the following systems: $13 + 13$, $34 + 34$, $50 + 50$, $100 + 100$ and $18 + 50$. The incident energies have been chosen in a way that the available energy in the center of mass frame ranges from an energy far below the binding energy of the fused system ($\approx 30 E.S.U.$) to an energy well above the binding

energy of the fused system ($\approx 120 E.S.U.$). As it will be shown, these collisions can be studied in the same way as the experimental data of nucleus-nucleus collisions are. These collisions can be seen as “numerical experiments”. Only few examples of such analyses will be shown. More detailed analyses will be done in forthcoming articles. Firstly, a small list of reaction mechanisms obtained will be done. Secondly, the excitation energy stored in excited clusters will be studied and a link to the static properties will be done. Finally, the question of the statistical description of this dynamical model will be briefly addressed.

A. Reaction mechanisms.

On figure 3 are displayed the pictures of cluster-cluster collisions obtained at a fixed time. The ending time

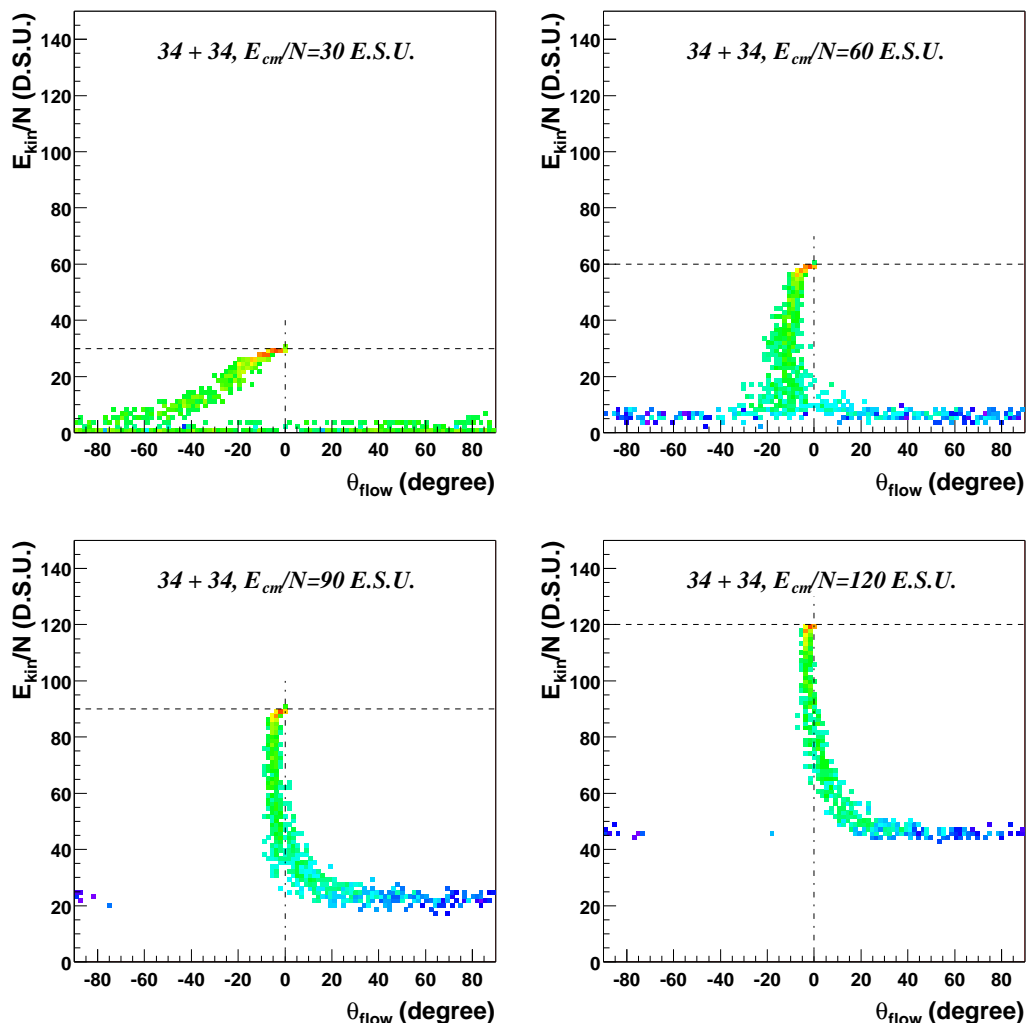


FIG. 4: Wilczynski plots for $N = 34 + N = 34$ collisions at different available energies in the center of mass (see text).

of these collisions is $t = 200 T.S.U.$. On each picture, the bodies which were originally belonging to the projectile are in dark grey and those which were belonging to the target are in light grey. The most striking observation is that all kinds of reaction mechanisms observed in nucleus-nucleus collisions seem to be present in this very simple simulation. One can see low energy processes like the fusion/evaporation process (first row left panel), pure binary collision (second row left panel), stripping/pick-up mechanism (second row right panel) and deep inelastic collisions (third row right panel). Intermediate energy processes, like neck formation and break-up (first row right panel) and multi-fragmentation (third row left panel), are seen. Finally, high energy processes like the participant/spectator process (lower-most panel) are also seen.

This similarity can also be seen on the so-called Wilczynski plots [26] shown on figure 4. These plots display the correlation between the flow angle θ_{flow} and the

total kinetic energy of the clusters $E_{kin} = \sum E_k^i$ where E_k^i is the kinetic energy of cluster i in the center of mass frame. Two bodies are assumed to belong to the same cluster if they are in interaction, i.e. if their relative distance is below the range r_1 of the interaction (see figure 1). This algorithm of cluster recognition is the simplest one and is called Minimum Spanning Tree algorithm in other works [22, 27]. The most dissipative collisions correspond to the smallest E_{kin} values: the available energy is converted in internal energy of clusters. These plots were built for a $N = 34$ projectile colliding a $N = 34$ target at four available energies E_{cm}/N in the center of mass: $E_{cm}/N = 60 E.S.U.$, $E_{cm}/N = 90 E.S.U.$, $E_{cm}/N = 120 E.S.U.$ and $E_{cm}/N = 30 E.S.U.$ which corresponds respectively to the energy of the less bound body for the fused $N = 68$ cluster, to the binding energy of the most bound body for $N = 68$ and to an energy below the energy of the less bound body for $N = 68$. For each energy,

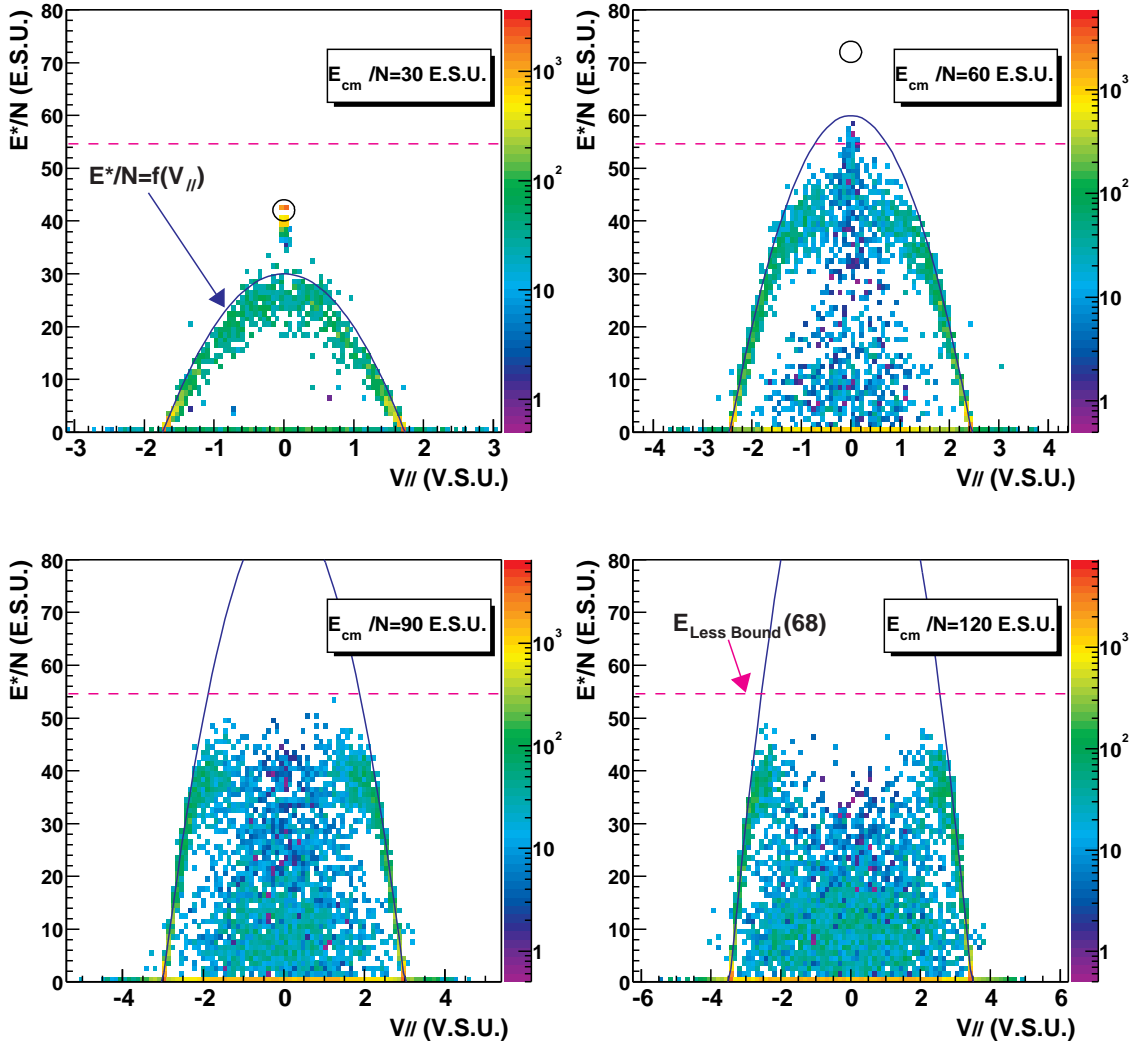


FIG. 5: Excitation energy of clusters versus their parallel velocity for $N = 34 + N = 34$ collisions at different available energies in the center of mass. On each panel, the full line corresponds to the expected evolution for a pure binary process, the dashed horizontal line corresponds to the energy of the less bound body for $N = 68$ and the circle corresponds to the expected values for the fused system.

1,000 collisions have been computed assuming a flat impact parameter distribution ranging from $b = 0 D.S.U.$ to the sum of the two cluster radii plus the range of the interaction ($b_{max} = r(N_{proj}) + r(N_{targ}) + r_1$, where r_1 is the range of the two-body interaction). In the analyses, each collision is weighted assuming a triangular impact parameter distribution between 0 and b_{max} ($weight \propto b$).

At $E_{cm}/N = 30 E.S.U.$ (upper left panel), the flow angle is always negative. This means that the projectile and the target like clusters are deflected to the opposite direction relative to their original one. At this energy, the attractive part of the interaction is dominant. For the lowest E_{kin} values, all possible values of θ_{flow} are covered: this corresponds to the fusion/evaporation process. At $E_{cm}/N = 60 E.S.U.$ (upper right panel), the picture is changed and the range of θ_{flow} values is smaller

than for the previous energy: the repulsive part starts to act. The fusion/evaporation area (small E_{kin} values, all θ_{flow} values) is still present. For the two highest energies (lower panels), the picture is roughly the same. For the less dissipative collisions, the attractive part is still dominant (negative θ_{flow} values). But when the dissipation increases, the repulsive part becomes dominant and the projectile and the target bounce on each other (positive θ_{flow} values). For the most dissipative collisions, only positive θ_{flow} values are seen which indicates the disappearance of the fusion/evaporation process. These evolutions are qualitatively similar to what is seen in nucleus-nucleus collisions (see for example [28]).

These two studies indicate that the description of the reaction mechanisms in terms of mean-field at low energies and in terms of nucleon-nucleon collision at high en-

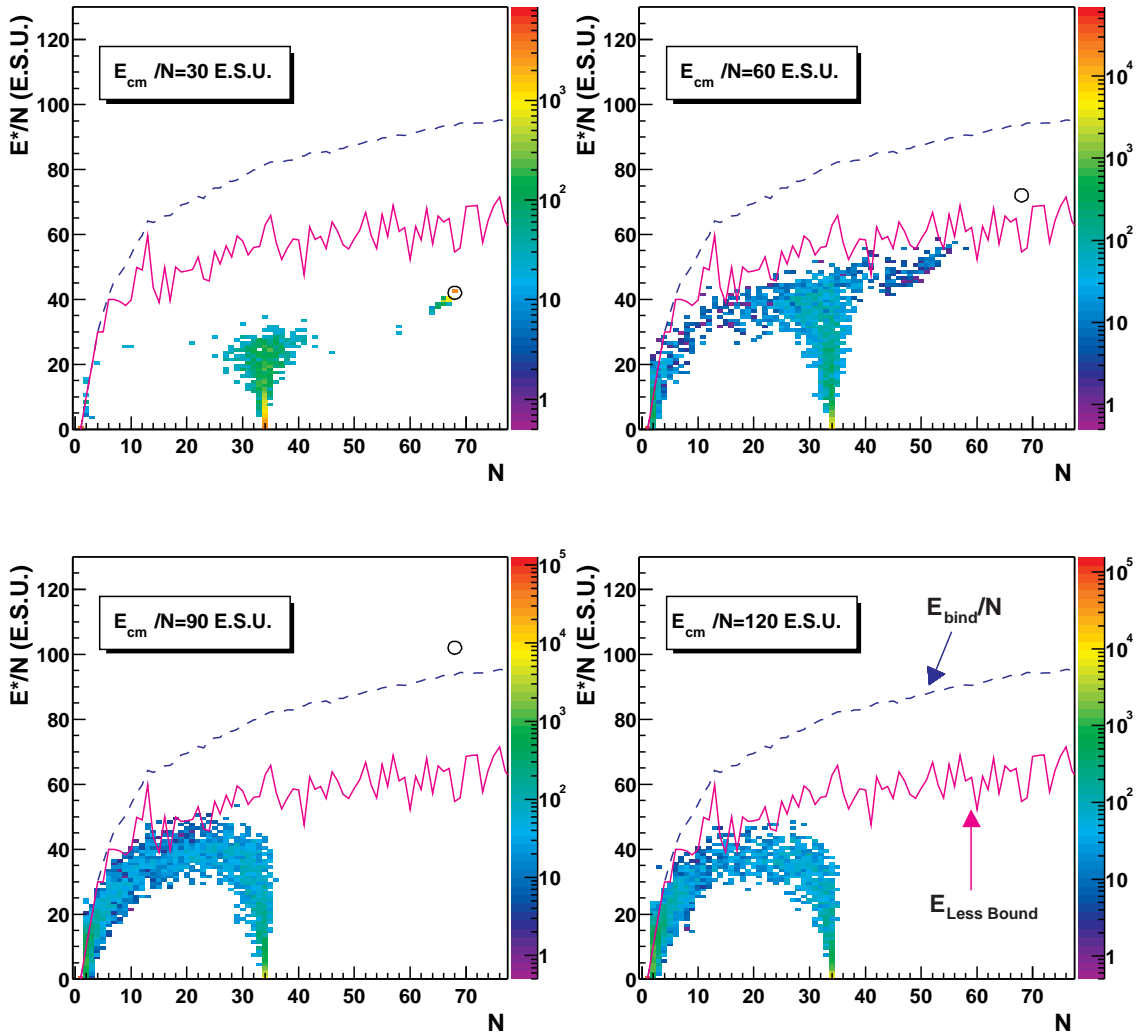


FIG. 6: Excitation energy of clusters versus N for $N = 34 + N = 34$ collisions at different available energies in the center of mass. On each panel, the full line corresponds to the energy of the less bound body, the dashed line corresponds to the binding energy per body and the circle corresponds to the expected values for the fused system.

ergies can be deduced from the properties of the nucleon-nucleon interaction only. The similarities of this classical N -body simulation with nucleus-nucleus collisions suggest that, apart for the quantum mechanics effects, an effective description of nucleus-nucleus collisions could be obtained with a reduced number of parameters. Providing the interaction has a finite range attractive part and a short range repulsive part, the overall behavior of the N -body systems seems to be independent of the values of the parameters of this interaction. For a more quantitative agreement with nucleus-nucleus collisions, additional physical ingredients (quantum mechanics, Coulomb interaction) have to be included.

B. Energy deposit in clusters.

Let us now focus our study of cluster-cluster collision on selected topics. Of particular interest is the excitation energy stored in clusters. How this energy can be linked to the available energy and how it is linked to the properties of the “ground state” characteristics of these clusters?

One can plot for example the evolution of the excitation energy E^*/N of the cluster with its parallel velocity $V_{//}$ for $N = 34 + N = 34$ collisions (figure 5) for the whole impact parameter range. The excitation energy of each cluster is simply the difference between the total energy (potential plus kinetic) and the “ground state” energy of the cluster. It reads:

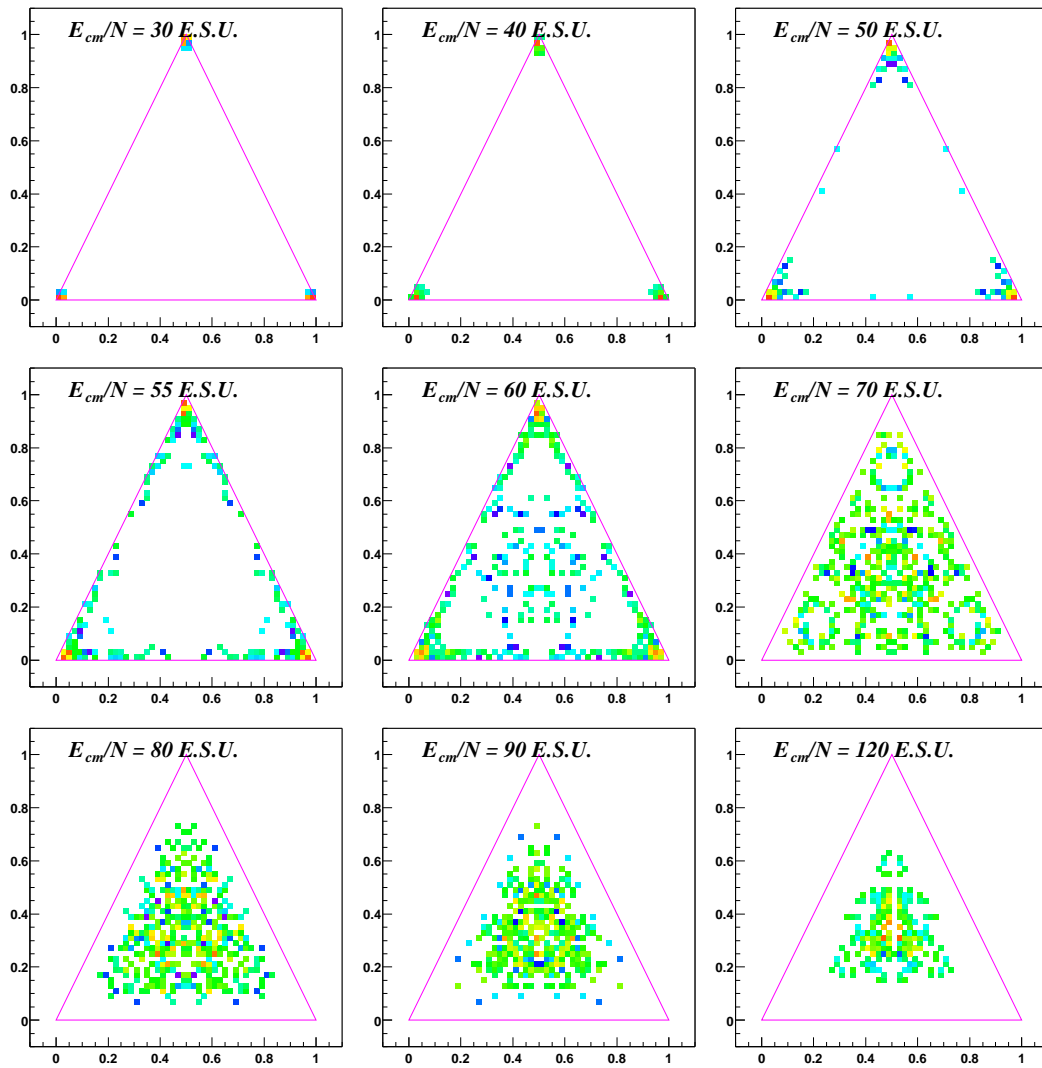


FIG. 7: Dalitz plots for CNBD simulations for central ($0 \leq b/b_{max} < 0.1$) $N = 34 + N = 34$ collisions at different available energies in the center of mass.

$$E^* = \sum_{i=1}^N E_{kin}^i + \sum_{i,j>i} V(r_{ij}) - E_{Bind}(N) \quad (1)$$

where E_{kin}^i is the kinetic energy of the body i in the cluster center of mass frame, r_{ij} the relative distance between the bodies i and j , $V(r_{ij})$ the potential energy and $E_{Bind}(N)$ the binding energy of the “ground-state” of the cluster with N bodies. This excitation energy is determined at the end of the calculation corresponding to $t = 200 T.S.U.$. This energy is very close to the one obtained at the separation time of the clusters (the smallest time at which clusters can be identified), since in this time range the evaporation is very weak and the clusters have no time to cool down significantly [22]. On each panel of figure 5, the full line corresponds to the

expected correlation between E^*/N and $V_{//}$ for a pure binary scenario (the excitation energy is only due to the velocity damping of each partner), the horizontal dashed line to the energy of the less bound body for the fused system $N = 68$ and the small circle is centered around the expected values of velocity and excitation energy for the fused system.

At $E_{cm}/N = 30 E.S.U.$, the points are slightly below the full line. This means that the excitation energy is strongly linked to the velocity damping. The small shift is due to mass transfers between the projectile and the target, and to promptly emitted clusters. The area corresponding to the fused system is well populated showing that a complete fusion process occurs. At $E_{cm}/N = 60 E.S.U.$, the distribution of points is roughly compatible with the pure binary process hypothesis, but the complete fusion process area is empty. The horizontal

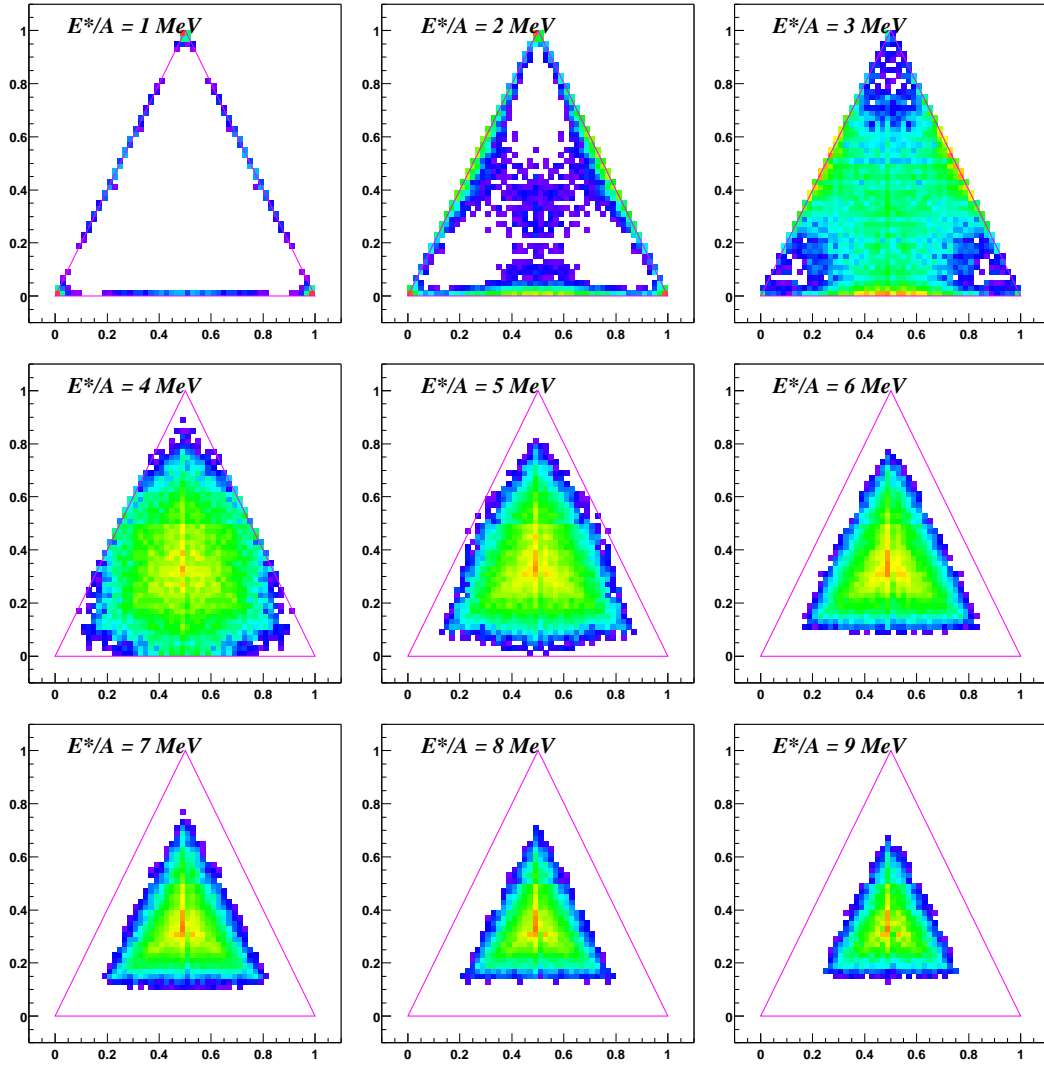


FIG. 8: Dalitz plots obtained with SMM calculations for different excitation energies. The source has a charge $Z = 86$, a mass $A = 205$ and the freeze-out density is $\rho_{f.o.} = \rho_0/3$.

line seems to be an upper limit to the excitation energy which can be stored in clusters. Clusters with rather small excitation energies are found at velocities around the center of mass velocity. For the two highest energies, this trend is enhanced: a set of clusters are around the full line, and when the full line is above the horizontal line, one finds clusters at small excitation energies around the center of mass velocity. The energy of the less bound body seems to be a limit to the excitation energy which can be stored in these clusters.

This can be more clearly seen when the excitation energy E^*/N is plotted as a function of N , as in figure 6. On each panel, the full line corresponds to the energy of the less bound body $E_{LessBound}$ in the cluster and the dashed line to the binding energy per body E_{bind}/N . As in figure 5, the small circle corresponds to the expected values for the fused system. At $E_{cm}/N = 30 E.S.U.$,

the area corresponding to complete fusion is filled and all the available energy can be stored as excitation energy. But for higher energies, one can clearly see that for each fragment size, E^*/N never overcomes $E_{LessBound}$. At $E_{cm}/N = 60 E.S.U.$ clusters with sizes higher than the projectile size and the target size can be seen. This area corresponds to an incomplete fusion process. For the two highest energies ($E_{cm}/N = 90 E.S.U.$ and $E_{cm}/N = 120 E.S.U.$), the plots are almost identical: there is no more fusion and the clusters are smaller than the target and than the projectile. One can notice that E^*/N never reaches the binding energy E_{bind}/N except for small clusters where E_{bind}/N and $E_{LessBound}$ are equal.

This limitation of excitation energy can be understood quite easily. The less bound body remains bound to the cluster only if its total energy is negative, i.e. its kinetic energy due to the excitation is below its potential one. If

one assumes that the excitation energy is roughly equally shared over all bodies in the cluster, when the kinetic energy balances the potential energy of the less bound body, this body is no more bound to the cluster and can escape. To be observed for a long time, the excited cluster must have an excitation energy per body below the energy of the less bound body.

The mechanism of energy deposit in classical N-body clusters seems to be the following one: the excitation seems to be mainly driven by the velocity damping of the two partners and to a lesser extent by exchanges of bodies between them. Once the energy of the less bound body is reached, unbound bodies and/or clusters escape quickly and keep an excitation energy per body below the energy of the less bound one. As a consequence, the highest energy deposit per body can only be obtained at energies close to $E_{LessBound}$. For higher available energies, the system fragments quickly, leaving rather “cold” clusters around the center of mass velocity. This could be an explanation to the quite low excitation energies of clusters found in central collisions for the Xe + Sn system at 50 A.MeV [29]. This subject will be more completely covered in a forthcoming article.

C. Statistical description of collisions.

Let us end with fragment size analyses of cluster-cluster collisions. In nucleus-nucleus collisions studies, such analyses are very often used to fix the parameters of statistical models and to verify the compatibility of statistical decay models with experimental data (see for example [30, 31, 32]). The so-called Dalitz plot for central ($0 \leq b/b_{max} < 0.1$) $N = 34 + N = 34$ collisions are shown on figure 7. Each panel corresponds to a fixed available energy in the center of mass ranging from $E_{cm}/N = 30$ to $120 E.S.U.$. For this analysis, only the three heaviest clusters are taken into account. Each event is associated with a point in this plot. The distance of one point with respect to each edge of the triangle is proportional to the size of each of the three clusters. The corners correspond to events with a large size cluster and two small ones (fusion/evaporation process), an event in the middle of an edge corresponds to an event with two equal size clusters and a small one (fission process or binary collision) and the center of the triangle corresponds to three equal size clusters (multi-fragmentation process). One can see that when the available energy increases, the reaction mechanisms goes continuously from fusion/evaporation to binary collisions and finally to multi-fragmentation and/or vaporization.

This picture is qualitatively very similar to the one obtained in SMM calculations [12], describing the decay of a single source, as shown on figure 8. In this case, each panel corresponds to an excitation energy. As in figure 7, the lowest energies correspond to fusion/evaporation like processes, and goes with a continuous transition towards

fission and multi-fragmentation when the excitation energy increases.

The strong qualitative similarity between these two pictures suggests that it could be possible to build a statistical decay code which would give the same results as the dynamical simulation. Of particular interest would be the study of the relations between the parameters of the statistical decay code (size of the source, excitation energy, deformation, radial flow, freeze-out volume, external constraints) with the parameters of the dynamical one (projectile and target sizes, impact parameter, parameters of the two-body interaction). This could also allow to check under which conditions the statistical decay code can be applied. This study could finally allow us to have a consistent description of cluster-cluster collisions, where the parameters of the statistical decay model are deduced from the parameters of the dynamical simulation. In this case, the cluster-cluster collisions could be described completely with a reduced number of parameters.

IV. CONCLUSIONS

As it has been seen in this brief overview of the characteristics and the reaction mechanisms of classical N bodies in strong interaction, there are strong qualitative similarities between these systems and the atomic nuclei. The static properties and the reaction mechanisms observed for the atomic nuclei and for these classical clusters are found very close to each other. This could mean that the experimental observations made for nucleus-nucleus collisions are mainly governed by the N-body character of the system and by the overall shape of the two-body interaction (finite range attractive part and short range repulsive part). More physical ingredients (Coulomb interaction, quantum mechanics) are of course necessary if one wants to have a quantitative agreement with experimental data. But it is surprising to have such a qualitative agreement while essential physical ingredients are missing in the simulation.

Since all kind of reaction mechanisms are observed in these classical simulations, from the low energy fusion/evaporation processes to the high energy participant/spectator processes, they may also allow to connect in a consistent way the mean-field and the nucleon-nucleon approaches. One could for example study the relation between the incompressibility modulus and the size of the repulsive part of the interaction (K_∞ and σ_{nn} in the nuclear case). It is well known in transport calculations that one can “stiffen” the effective equation of state by just increasing the value of the nucleon-nucleon cross section σ_{nn} [33].

Finally, such simulations may reconcile two approaches which were up to now opposed in nuclear physics: the dynamical description and the statistical description of fragment emissions. The dynamical models are unique tools to establish the link between the parameters of the inter-

action and those of the statistical models. Additionally, one can determine under which conditions the statistical models can be used, and what are the true meanings of the parameters used in statistical models (temperature, chemical potentials, freeze-out volumes, etc.). This study may allow to have a complete and consistent description of colliding N-body systems with a reduced number of free parameters. This could be not only useful for nuclear physics, but also for other fields of physics like for example the cluster physics.

Acknowledgments

I would like to thank my colleagues of the INDRA collaboration and from the Laboratoire de Physique Corpusculaire de Caen for a careful reading of this article. I especially thanks Denis Lacroix for suggestions and fruitful discussions. I would like also to thank O.Lopez and A.Botvina for the SMM calculations.

-
- [1] S.E.Koonin, Prog. in Part and Nuc. Phys. **Vol. 4** , 283 (1979).
- [2] J.Cugnon *et al.*, Nucl. Phys. **A352** , 505 (1981).
- [3] C.Grégoire *et al.*, Nucl. Phys. **A465** , 317 (1987).
- [4] A.Bonasera *et al.*, Physics Report **243** , 1 (1994).
- [5] G.Bertsch, Phys. Rev. **C29** , 673 (1984).
- [6] S.Ayik and C.Grégoire, Nucl. Phys. **A513** , 187 (1990).
- [7] J.Aichelin, Physics Report **202** , 233 (1991).
- [8] A.Ono *et al.*, Phys. Rev. **C48** , 2946 (1993).
- [9] H.Feldmeier, Nucl. Phys. **A428** , 147 (1990).
- [10] R.Charity *et al.*, Nucl. Phys. **A511** , 59 (1990).
- [11] D.Durand, Nucl. Phys. **A541** , 266 (1992).
- [12] J.Bondorf *et al.*, Phys. Rep. **257** , 133 (1995).
- [13] D.H.E.Gross, Rep. Prog. Phys. **53** , 605 (1990).
- [14] J.Konopka *et al.*, Phys. Rev. **C50** , 2085 (1994).
- [15] W.Friedman, Phys. Rev. **C42** , 667 (1990).
- [16] T.J.Schlagel and V.R.Pandharipande, Phys. Rev. **C36** , 162 (1987).
- [17] C.Dorso and J.Randrup, Phys. Lett. **B215** , 611 (1988).
- [18] V.Latora *et al.*, Nucl. Phys. **A572** , 477 (1994).
- [19] J.Bondorf *et al.*, Nucl. Phys. **A624** , 706 (1997).
- [20] X.Campi, H.Krivine and N.Sator, Nucl. Phys. **A681** , (2000).
- [21] E.Plagnol *et al.*, *Proceedings of the XXXIX International Winter Meeting on Nuclear Physics*, Edited by I.Iori, (2001).
- [22] A.Strachan and C.Dorso, Phys. Rev. **C59** , 285 (1999).
- [23] W.H.Press, B.P.Flannery, S.A.Teukolsky and W.T.Vetterling. *Numerical Recipes*. Cambridge University Press (1989).
- [24] C.Dorso, S.Duarte and J.Randrup, Phys. Lett. **B188** , 287 (1987).
- [25] D.J.Wales and J.P.K.Doye, J. Phys. Chem. **A101** , 5111 (1997).
- [26] J.Wilczynski, Phys. Lett. **B47** , 313 (1973).
- [27] C.Dorso and J.Randrup, Phys. Lett. **B301** , 328 (1993).
- [28] V.Métivier *et al.* (INDRA Collaboration), Nucl. Phys. **A672** , 357 (2000).
- [29] N.Marie *et al.* (INDRA Collaboration), Phys. Rev. **C58** , 256 (1998).
- [30] N.Marie *et al.* (INDRA Collaboration), Phys. Lett. **B391** , 15 (1997).
- [31] M.D'Agostino *et al.*, Nucl. Phys. **A650** , 329 (1999).
- [32] F.Bocage *et al.* (INDRA Collaboration), Nucl. Phys. **A676** , 391 (2000).
- [33] V.De La Mota, F.Séville, M.Farine, B.Remaud and P.Schuck, Phys. Rev. **C46** , 677 (1992).